Received: 11 July 2017 | Revised: 10 September 2017 | Accepted: 16 October 2017

DOI: 10.1002/rcm.8020

WILEY Rapid Communications in Mass Spectrometry

RESEARCH ARTICLE

High-precision determination of lithium and magnesium isotopes utilising single column separation and multi-collector inductively coupled plasma mass spectrometry

Madeleine S. Bohlin[1] | Sambuddha Misra[1,2] | Nicholas Lloyd[3] | Henry Elderfield[1†] | Mike J. Bickle[1]

[1] Department of Earth Sciences, University of Cambridge, Downing Street, Cambridge CB2 3EQ, UK

[2] Centre for Earth Sciences, Indian Institute of Science, Bangalore 560012, India

[3] Thermo Fisher Scientific, Hanna-Kunath-Str. 11, 28199 Bremen, Germany

Correspondence
M. S. Bohlin, University of Cambridge, Department of Earth Sciences, Downing Street, Cambridge CB2 3EQ, UK.
Email: msb56@cam.ac.uk

Funding information
FP7 People: Marie-Curie Actions, Grant/Award Number: 316966; European Research Council, Grant/Award Number: 2010-NEWLOG ADG-267931; Natural Environment Research Council, Grant/Award Numbers: NE/P011659/1 and NE/N007441/1

Rationale: Li and Mg isotopes are increasingly used as a combined tool within the geosciences. However, established methods require separate sample purification protocols utilising several column separation procedures. This study presents a single-step cation-exchange method for quantitative separation of trace levels of Li and Mg from multiple sample matrices.

Methods: The column method utilises the macro-porous AGMP-50 resin and a high-aspect ratio column, allowing quantitative separation of Li and Mg from natural waters, sediments, rocks and carbonate matrices following the same elution protocol. High-precision isotope determination was conducted by multi-collector inductively coupled plasma mass spectrometry (MC-ICPMS) on the Thermo Scientific™ NEPTUNE *Plus*™ fitted with 10^{13} Ω amplifiers which allow accurate and precise measurements at ion beams ≤0.51 V.

Results: Sub-nanogram Li samples (0.3–0.5 ng) were regularly separated (yielding Mg masses of 1–70 μg) using the presented column method. The total sample consumption during isotopic analysis is <0.5 ng Li and <115 ng Mg with long-term external 2σ precisions of ±0.39‰ for δ^7Li and ±0.07‰ for δ^{26}Mg. The results for geological reference standards and seawater analysed by our method are in excellent agreement with published values despite the order of magnitude lower sample consumption.

Conclusions: The possibility of eluting small sample masses and the low analytical sample consumption make this method ideal for samples of limited mass or low Li concentration, such as foraminifera, mineral separates or dilute river waters.

1 | INTRODUCTION

Lithium and magnesium stable isotope geochemistry has the potential to provide insights into low- and high-temperature geological processes such as weathering of the continental and oceanic crust (e.g.[1-10]), cycling of material through the crust and mantle (e.g.[11-15]) and cosmochemical processes (e.g.[16-18]). The large relative mass difference between the stable isotopes of both Li and Mg (~16% difference in mass between ^{7}Li and ^{6}Li, and ~8% between ^{26}Mg and ^{24}Mg) leads to significant isotope fractionation during physical and chemical reactions,[19] making both elements sensitive tracers for geochemical processes (e.g.[20,21]). However, significant mass-dependent isotope fractionations may occur during chemical purification and mass spectrometric measurements. It is therefore essential to avoid isotopic fractionation during chemical purification and to make appriate corrections for fractionation during analysis.

Isotope ratio determination of Li and Mg is achieved by multi-collector inductively coupled plasma mass spectrometry (MC-ICPMS). Due to potential isobaric interferences from doubly charged species generated in the plasma, and the effect of other matrix elements on

[†] Deceased.

the instrumental mass bias, it is necessary to analyse purified mono-elemental solutions (e.g.[22-24]). This requires a multi-step sample preparation, including the separation of Li and Mg from sample matrix through cation-exchange chromatography. Lithium has previously been separated by using between one and four separate column procedures (e.g.[23,25-27]) whereas Mg is eluted in two or three columns (e.g.[4,18,28]). The objective of analysing both Li and Mg on the same sample would thus require between three and seven separate column procedures. This approach is time-consuming and increases sample blanks and the risk of incomplete sample recovery with associated isotopic fractionation.

In this paper we present a single column, one-step elution method to separate small masses of Li and Mg from multiple sample matrices. Seawater, river water, sediment, foraminifera and rock standards with established isotopic compositions have been processed, with Li and Mg column loads varying between 0.3 and 20 ng for Li and between 1 and 70 μg for Mg to demonstrate the robustness of the method. Our technique utilises the Thermo Scientific™ NEPTUNE *Plus*™ MC-ICPMS instrument (Thermo Scientific, Bremen, Germany) with 10^{13} Ω amplifiers, allowing sub-nanogram samples of Li to be measured with high external precision (±0.39‰, 2σ), and consuming less than 0.5 ng per duplicate analysis. Mg isotopes are measured with 10^{11} Ω amplifiers consuming less than 115 ng Mg per duplicate analysis with a long-term external precision of ±0.07‰ (2σ).

2 | EXPERIMENTAL

2.1 | Sample and standard preparation

All acids used in this study (reagent grade, Fisher Scientific, Loughborough, UK) were doubly distilled in a Teflon sub-boiling still and prepared to the required molarity using 18.2 MΩ Milli-Q water (Millipore, Watford, UK). The molarity of the hydrochloric acids used for column separation (0.70 N, 1.50 N and 10 N) was confirmed by titration using 1.0 M certified grade NaOH (Fisher Scientific).

Samples used in this study were prepared as follows. Seawater and river water samples were evaporated to dryness at 80°C and then refluxed with 1–2 mL of concentrated aqua regia at 100°C overnight to oxidise organic matter. The samples were then evaporated to dryness and taken up in 0.7 N HCl to be loaded onto the ion-exchange column. Sediment and rock powders were baked at 950°C for 8 h in ceramic crucibles to destroy organic matter, and then dissolved in a mixture of concentrated HNO_3, HCl and HF (1:1:1) in Savillex© (Eden Prairie, MN, USA) screw-top beakers on a hotplate at 110°C. Post dissolution (typically a few hours), the samples were dried down and taken up in 6 N HCl. If fluoride residues were present the sample was refluxed with concentrated HNO_3 until a clear solution was obtained. An aliquot, generally containing 1–10 ng Li, was then diluted to 200 μL with 0.7 N HCl and loaded onto the columns. The synthetic foraminifera standard was made from pure concentrated stock solutions (ROMIL-SpS™ super purity standards, Waterbeach, UK). The column loads of different elements for each sample matrix that were utilised to generate the column elution/calibration curves (Figure 1) are presented in Table 1.

2.2 | Column chromatography

Sulphonated polystyrene cation-exchange resins have a high load capacity (~1.7 mEq/mL dry resin) and micro-porous gel-type resins, such as AG50W-X8 and AG50W-X12 (BioRad™), are traditionally used for the chromatographic separation of Li and Mg (e.g.[4,23,24,27]). However, the distribution coefficients for Li and Na, and those of Mg, Fe and Mn, for different strength acids and the AG50W resin are similar, especially with increasing acid strength (Table 2).[29] Therefore, dilute acids and/or a combination of several columns are commonly utilised to fully separate both Li and Mg from other matrix elements (e.g.[4,27,28]). Alternatively, a mixture of dilute HCl or HNO_3 and an organic solvent also increases the separation especially between Li and Na (e.g.[25,26,31,32]). However, organic solvents and HNO_3 may cause: (1) rapid degradation of the resin resulting in non-quantifiable migration of element peaks; (2) early breakthrough of Na into the Li fraction;[30,31] and (3) rapid volatilisation of methanol, which has been hypothesised to cause element peak migration and cross contamination of Li between columns.[32] Other strategies include initial removal of Fe from high Fe matrices by eluting through an anion-exchange column, reducing the total matrix load.[15,18,33] The

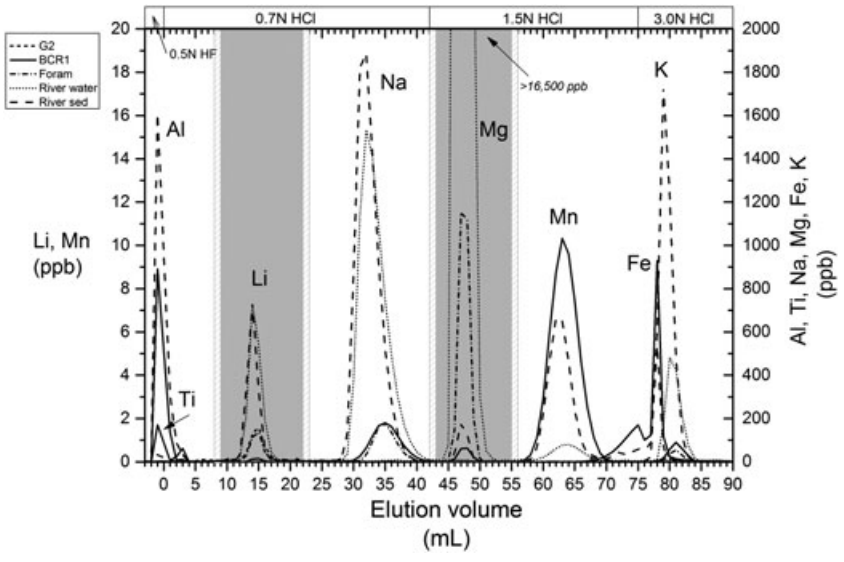

FIGURE 1 Elution curves for various sample matrices: G2 granite (short-dashed line – only Li), BCR-1 basalt (solid line), foraminifera calcite standard (dashed dotted line), river water (dotted line) and river sediment (dashed line). For samples with high Al and Ti load, the initial 3 mL are eluted in 0.5 N HF, and the elution volume (x-axis) denotes the volume of HCl added. The grey boxes mark the cuts which are collected for Li and Mg isotope analysis, with the 1-mL pre- and post-cuts in grey stripes. The calibration was carried out volumetrically by collection of each millilitre of the elution. Ca, Sr and Ba elute after 100 mL. (For sample composition, see Table 1)

TABLE 1 Loaded masses on column for calibration seen in Figure 1

		Sample/matrix				
Element	unit	Himalayan river water	Himalayan river sediment	BCR-1 (basalt)	G2 (granite)	Foraminifera standard
Al	µg	44.5 (ng)	17.4	4.0	24.0	-
Ca	µg	74.5	2.3	2.8	4.1	770.0
Mg	µg	30.2	0.8	1.2	1.3	3.5
K	µg	3.3	8.6	0.8	10.9	0.7
Li	ng	20.0	20.0	0.5	10.0	7.0
Na	µg	7.3	7.6	1.3	8.9	1.8
Mn	ng	2.9	68.4	84.4	68.2	70.0
Ti	ng	2.5	315.2	750.0	852.9	-
Fe	µg	11.8 (ng)	2.9	5.4	5.5	0.1
Li/Mg	µg/µg	6.6×10^{-4}	2.5×10^{-2}	4.2×10^{-4}	7.6×10^{-3}	2.0×10^{-3}
Li/Tot	µg/µg	1.7×10^{-4}	5.0×10^{-4}	3.1×10^{-5}	1.8×10^{-4}	9.0×10^{-6}

peak separation of Mg, especially from Fe and Mn, and that of Li from Na, is significantly larger in the macro-porous equivalent of the gel-type resin – AGMP-50 (BioRad™, Hercules, CA, USA)[34,35] (Table 2). Utilising a 3-mL Savillex® Teflon™ ion-exchange column with high aspect ratio (25 cm height and inner diameter of 4 mm), quantitative separation of both Li and Mg from multiple matrices is achieved in a single-step elution.

2.2.1 | Elution protocol

The resin was backwashed using a handheld pump and allowed to settle under gravity between each elution. This enables the resin to fully expand and uniformly distribute with homogeneous porosity between each sample elution. The columns were then conditioned with 9 mL (three column volumes) of 0.7 N HCl before being loaded with the sample (typically 2 ng Li yielding Mg masses between 1 and 70 µg). Samples were loaded in <200 µL of 0.7 N HCl, and then eluted with 9 mL of 0.7 N HCl, with the first 1 mL added incrementally in steps of 200 µL to ensure that the sample is properly loaded onto the resin. Li was then eluted in 0.7 N HCl and collected as a 13-mL cut. A 1-mL pre- and a post-Li cut were collected to ensure that there was no Na breakthrough and that the Li peak was contained within the 13-mL cut. Following collection of Li, the column was eluted with 18 mL of 0.7 N and an additional 1 mL of 1.50 N HCl. The Mg fraction was then collected in 12 mL of 1.50 N HCl, with a pre- and post-Mg cut of 1 mL collected before and after the Mg peak. Prior to reuse, the columns were washed with 15 mL of 10 N HCl and 15 mL of 18.2 MΩ Milli-Q water, and, depending on the loaded mass and type of sample, one more wash of 10 N HCl and water may be required, as divalent cations such as Ca, Ba and Sr are strongly retained by the AGMP-50 resin. The same elution protocol was used for all sample matrices, with an additional 3 mL of 0.5 N HF added immediately after sample loading for rock and sediment samples with significant (weight percentage) Al and Ti.[36] These elements may otherwise co-elute with Mg (Figure 2) but are eluted within the first few mL of dilute HF. The full elution protocol is presented in Table 3. Following column elution the Li and Mg cuts were dried down on a hotplate at 90°C before being refluxed for 24 h with concentrated double-distilled HNO_3. This converts the sample into a nitrate salt and oxidises any organic matter derived from possible resin degradation. The refluxed samples were dried down on the hotplate and were then taken up in 2% HNO_3 for analysis by MC-ICPMS.

TABLE 2 Distribution coefficients of selected elements with varying strength of HCl (0.5–2 N) for AGMP-50 resin utilised in this study, and the AG50W-X8 resin commonly used. Key differences include the larger separation between Li and Na, and that between Mg and Fe/Mn, using AGMP-50

Distribution coefficients at varying acid strength						
	AG MP-50[a]			AG 50 W-X8[b]		
	0.5 N HCl	1.0 N HCl	2.0 N HCl	0.5 N HCl	1.0 N HCl	2.0 N HCl
Sr	1320	320	83	-	60	17.8
Ca	850	214	57	151	41.3	12.2
Fe (III)	800	89	10	225	33.5	5.2
Mn	161	43.6	11.3	84	20.2	6
Fe(II)	113	30	6.9	66	19.8	4.1
Ni	108	27.4	6.8	70	21.9	7.2
Mg	89	24.8	7.2	74	20.1	6.2
Ti	37.8	10.7	3.9	39.1	11.9	3.7
K	69	34.9	17.1	29.1	13.9	7.2
Na	26	13.6	8.4	13.5	6.9	3.8
Li	9.8	5.1	3.3	8.1	3.8	2.5

[a]Values from Strelow.[34]

[b]Values from Strelow et al.[29]

The elution protocol was calibrated for several different sample matrices (Table 1; Figure 1). During calibration every mL of acid was collected and analysed for concentration of cations by optical emission spectrometry (ICP-OES, Agilent® 5100, Stockport, UK) and Li by ICP-MS (Thermo Scientific™ ELEMENT XR™).

2.3 | Mass spectrometry

High-precision isotope ratio determination of both Li and Mg was performed by MC-ICPMS at the University of Cambridge (Cambridge, UK) on the Thermo Scientific™ NEPTUNE *Plus*™ fitted with a Jet ion extraction pump. We adopted a concentration matched standard-sample bracketing technique to correct for instrumental drift and mass bias. Each standard and sample were followed by a background instrumental blank measurement in 2% HNO_3 matrix. A typical

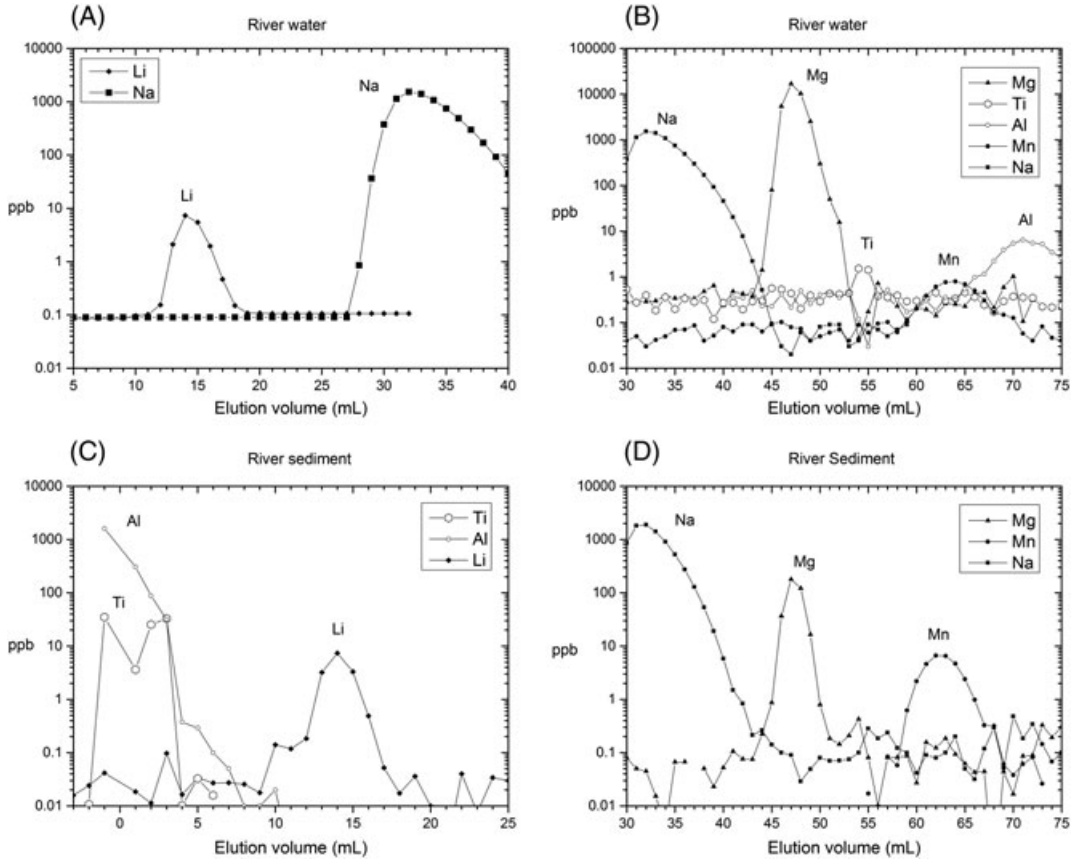

FIGURE 2 Separation of elements in the AGMP-50 resin utilising our elution protocol, with concentration in log-scale to magnify tailing of neighbouring elements for the river water matrix (A, B) and the river sediment matrix (C, D). Lithium is separated from Na with no peak-tail overlap. There is a minor (although insignificant given the high Mg concentrations) tailing of Na into the Mg peak. Samples that are not eluted with initial HF (e.g. water samples and foraminifera carbonate) have Ti and Al eluting after Mg (B), compared with prior to Li when HF is used (C). Ti concentrations are low in water samples and the tailing into Mg is negligible. Note that in (A) the average Na blanks from the pre-Na peak are plotted. Mg is clearly separated from Mn, Fe, and K (both Fe and K elute at >75 mL)

sequence consisted of the following measurements in the order of: blank-standard-blank-sample-blank-standard, with blank correction performed by subtracting the average of the blank measured before and after each sample and standard. Peak-centering was performed during each standard measurement. Both Li and Mg samples were measured in duplicate, with each measurement consisting of 33 cycles with 8.4 s integration time (total of 9 min 15 s sample analysis time) and an uptake time of 60 s.

TABLE 3 Elution protocol for single-step separation of Li and Mg from sample matrix

Elution cut		Volume	Reagent
	Backwash Condition	 ~ 9 mL	MQ 0.7 N HCl
E0	Load sample *(for sediments/rocks)*	200 µL *3 mL* 8 mL	0.7 N HCl *0.5 N HF)* 0.7 N HCl
E1	Pre-Li	1 mL	0.7 N HCl
E2	Li	13 mL	0.7 N HCl
E3	Post-Li	1 mL	0.7 N HCl
E4	Na	18 mL 1 mL	0.7 N HCl 1.5 N HCl
E5	Pre-Mg	1 mL	1.5 N HCl
E6	Mg	12 mL	1.5 N HCl
E7	Post-Mg	1 mL	1.5 N HCl
	Wash	15 mL 15 mL 15 mL 15 mL	10 N HCl MQ 10 N HCl MQ

2.3.1 | Li isotopic measurements

Li isotopic ratios were determined with respect to the NIST L-SVEC standard[37] and each analytical session included the measurement of secondary standards spiked with ^{6}Li and ^{7}Li (Li6-N and Li7-N, respectively[38]) to quantify external reproducibility. Measurements were performed using an APEX-IR (ESI®, Omaha, NE, USA) sample introduction system with a heated spray chamber set at 140°C and a Peltier cooling coil at 2°C. Additional details of the instrumental setup are presented in Table 4. The key feature of the δ^{7}Li determination method was the use of 10^{13} Ω amplifiers (Thermo Scientific) with ultra-low electronic noise that allowed determination of precise ^{7}Li/^{6}Li ratios with ^{6}Li and ^{7}Li beam sizes of ≤35 mV and ≤0.51 V, respectively. The low baseline noise of the 10^{13} Ω amplifiers (±0.9 µV, 1σ, n = 900) gave a 4- to 5-fold higher signal-to-noise ratio for ^{6}Li beam intensities of 15–35 mV than when using 10^{11} Ω amplifiers (±4.2 µV, 1σ, n = 900). Prior to each analytical session a long baseline of 900 cycles was performed. A Savillex® C-flow self-

TABLE 4 Instrumental parameters for the analysis of Li and Mg isotopes on the NEPTUNE *Plus*™

	Li	Mg
Preferred analyte concentration	0.4 ppb (0.4 V on ^{7}Li)	200 ppb (10 V on ^{24}Mg)
RF-power	1200 W	1200 W
Guard electrode	On	On
Spray chamber	APEX-IR (Quartz)	Single pass Scott (Teflon™)
Nebuliser aspiration rate	100 µL/min	50 µL/min
Injector	1.8 mm (Platinum)	1.8 mm (Platinum)
Sampler cone	X (Nickel)	X (Nickel)
Skimmer cone	Jet (Nickel)	Jet (Nickel)
Faraday cups	L4, H4	L1, C, H1
Amplifiers	10^{13} Ω	10^{11} Ω
Resolution	Low	Medium
Uptake time	60 s	60 s
Wash time	90 s	90 s
Blocks	1	1
Cycles	33	33
Integration time	8.4 s	8.4 s
Total analysis time per sample	554.4 s	554.4 s
Sample consumption	<0.5 ng	<115 ng
Matrix	2% HNO_3	2% HNO_3
Bracketing standard	L-SVEC	DSM-3
Secondary standard	Li6-N, Li7-N	Cambridge-1

For the Faraday cups, the letter L stands for Low mass cup, H for High mass cup and C for the Centre cup.

aspirating nebuliser (100 µL/min), nickel Jet type sample cone and X type skimmer cone were used. This instrumental setup resulted in a ~0.4 V signal on ^{7}Li, measured in the H4 cup, for a 0.4 ppb Li solution (preferred analyte Li concentration). With an uptake time of 60 s, the total sample consumption per duplicate analysis is less than 0.5 ng Li. Seawater analysed at 0.2 V yielded values indistinguishable from that analysed at 0.4 V having a total consumption of 0.2 ng Li. Lithium analysis by ICPMS techniques is plagued by rapid build-up of Li blanks, possibly due to deposition and subsequent ionisation of Li from the skimmer cone.[31,39] Our strategy was to minimise the deposition of Li by pre-coating the cones with alkali or alkaline earth elements.[39] Prior to sample analysis the cones were conditioned by aspirating a 10 ppm Na solution for ~10 min. Using this "coating" technique, the Li background generally ranged from <0.5 to 3 mV, approximately 0.1–0.75% of the sample signal intensity. Without utilising the Na wash, the Li backgrounds could increase to ~100 mV, rendering it impossible to measure Li at the desired low concentration. In addition, nickel cones were preferred over platinum cones in the present study, as the latter suffered from higher and more rapidly increasing background levels, possibly due to less efficient Na-coating on the platinum.

2.3.2 | Mg isotopic measurements

The ratio of the three isotopes of Mg (*viz*: ^{24}Mg, ^{25}Mg and ^{26}Mg) were determined and bracketed against the DSM-3 standard.[40] Each analytical session contained the Cambridge-1 Mg secondary standard to quantify the external reproducibility of our instrumental method. Mg isotope ratios were determined under wet plasma conditions as published work highlights that dry plasma methods may be more sensitive to residual matrix elements in the analyte (e.g.[15,22,42,43]). A self-aspirating Savillex® C-flow 50 µL/min nebulizer, single pass Scott-type Teflon spray chamber, and nickel Jet type sample cone and X type skimmer cone were used (Table 4). A 200 ppb Mg solution gave a ~10 V signal on ^{24}Mg in medium resolution with this instrumental setup, giving a total sample consumption of less than 115 ng Mg per duplicate measurement.

3 | RESULTS

3.1 | Chromatographic separation of lithium and magnesium

Lithium and magnesium are quantitatively separated from elements such as Na, K, Al, Ti, Mn, Fe, Ca, Sr and Ba by our column elution protocol using the AGMP-50 resin. There is a 10 mL separation between Li and Na for Li masses ranging from 0.3 to 20 ng (Figure 1). The high Mg and Fe load for certain samples (e.g. basalts) appears to have an effect on the Li peak, as observed in previous studies.[27] However, this occurs when the loaded Li mass is above 5 ng. Basalt samples were therefor eluted with <2 ng Li. In general, element peaks are broader for higher sample loads (Figure 1). However, the high degree of separation between different elements enables larger cuts to be collected without contamination from adjacent elements. This allowed us to follow the same protocol for all the sample matrices tested in this study. This single elution method also quantitatively separates Fe and Mn from Mg. The 1-mL aliquots collected before and after the Li and Mg cuts were dried down and taken up in 2% HNO_3 and measured by MC-ICPMS on the Neptune instrument against a bracketing standard of known concentration to

confirm the absence of peak tailing of Li and Mg. The pre- and post-cut aliquots have concentrations of Li and Mg indistinguishable from those in the 2% HNO_3 blank acid, confirming the quantitative recovery of the analyte within the sample aliquot. Quantitative separation is vital as mass-dependent fractionation occurs within the column (e.g.[23,25,27,32,44]), resulting in ±200‰ fractionation of Li in our columns (Figure 3). The procedural blanks are <4 pg Li in the collected Li cut, and <1 ng Mg in the Mg cut (n = 6), ~10^{-3} and ~10^{-4} of the average loaded sample masses, respectively. The blank was measured by following the column procedure, and all subsequent post-column steps, with a blank sample. The entire cut (13 mL for Li and 12 mL for Mg) was dried down and taken up in 1 mL 2% HNO_3, and measured on the Neptune in concentrated form. The concentrated solutions yielded ^{7}Li intensities between 3 and 4 mV (corresponding to <4 pg of Li in the cut), which is ~4 times higher than the instrument background during the measurement. The concentrated Mg cuts yielded ^{24}Mg intensities between 40 and 45 mV corresponding to <1 ng of Mg.

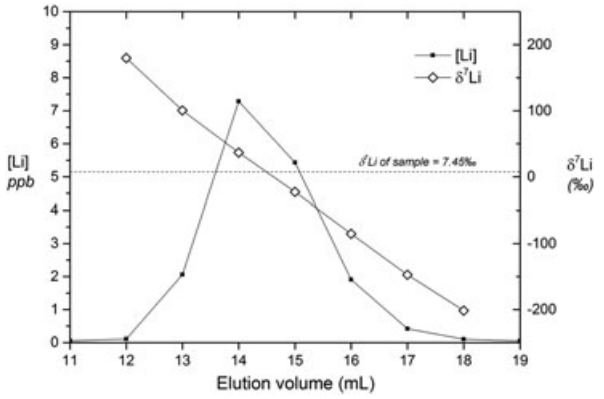

FIGURE 3 Fractionation of Li isotopes during elution of river water matrix (with δ^7Li value of 7.45‰) through the high aspect ratio column packed with AGMP-50 resin. The total fractionation is ±200‰. The figure illustrates the importance of quantitative recovery of the analyte during column elution

3.1.1 | Peak tailing of elements with similar distribution coefficients into the Li and Mg peaks

For rock and sediment samples, the addition of dilute HF (3 mL 0.5 N HF) to the elution protocol elutes Al and Ti in the first few millilitres (Figure 2C), effectively removing a large fraction of the total matrix load. Samples not eluted with HF, such as river water and foraminifera, have Ti and Al eluting after Mg, with Ti possibly overlapping with Mg (Figure 2B). However, the concentration of Ti in river water is negligible and there are thus no detectable amounts of Ti, especially after further dilution for Mg isotope analysis. There is a slight asymmetry in the Na-peak visible on a log-scale (Figures 2A and 2B). The Na tailing does not drastically change between sample matrices, with similar magnitudes observed for river water samples and seawater with

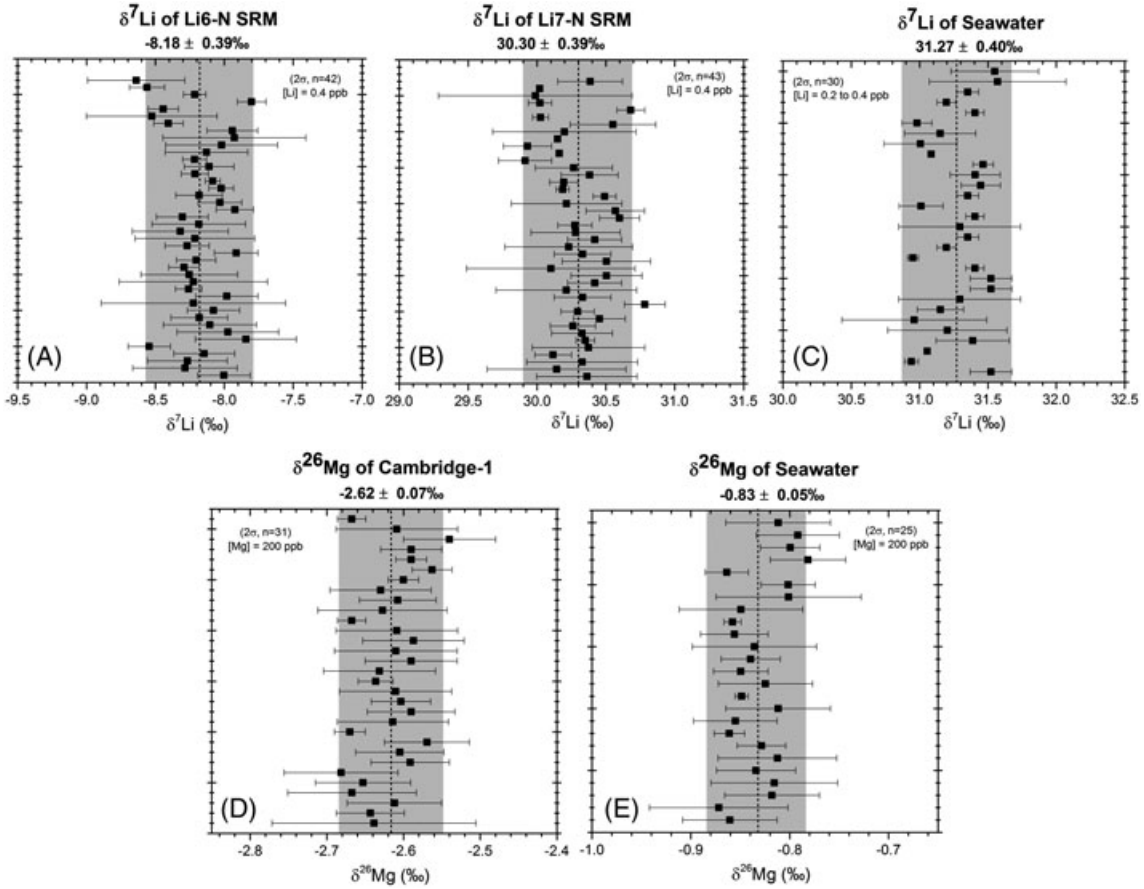

FIGURE 4 Long-term reproducibility of measured δ^7Li values of (A) Li6-N (−8.18 ± 0.39‰, *n* = 42) and (B) Li7-N (30.30 ± 0.39‰, *n* = 43) and δ^{26}Mg values of (D) Cambridge-1 (−2.62 ± 0.07‰, *n* = 31) measured during the course of 18 months. Seawater has been eluted through the columns and analysed for (C) δ^7Li values (31.27 ± 0.40‰, *n* = 30) and (E) δ^{26}Mg values (−0.83 ± 0.05‰, *n* = 25). The grey bands show the 2 standard deviations of the long-term mean of the sample population

Na/Mg ratios ~0.25 and ~8, respectively. The Na tailing leads to co-elution of a few ng of Na in a ~30 µg Mg peak, which is insignificant as it is further diluted by a factor of <150 before isotopic analysis on the Neptune mass spectrometer. The tailing can, however, be pronounced if the resin is not properly cleaned between successive sample passes.

3.2 | Isotope ratio determination by MC-ICPMS: Analyses and reproducibility of standards

The analytical fidelity of the isotope ratios of Li and Mg is dependent on their effective chromatographic separation, on appropriate reduction of the MS data, interferences and matching of sample and standard intensities and on reduction of concentrations of elements which affect mass bias. The presentation of results below evaluates the analytical protocols in terms of the potential impact on the measured isotopic ratios and confirms their effectiveness by analysis of standard reference materials.

The isotopic ratios of Li and Mg are expressed in the δ-notation (‰) by the convention:

$$\delta^{H}X = \left[\left(\frac{{}^{H}X/{}^{L}X_{sample}}{{}^{H}X/{}^{L}X_{standard}}\right)-1\right]\times 1000$$

where X is either Li or Mg, H is the heavy isotope and L the light isotope. Lithium samples are normalised to NIST SRM 8545 L-SVEC and Mg to DSM-3. Long-term average δ^{7}Li values of Li6-N and Li7-N secondary standards are −8.18 ± 0.39‰ (2σ, *n* = 42) and 30.30 ± 0.39‰ (2σ, *n* = 43), respectively (Figure 4). These are within the range of reported values of −8.9 to −8‰ and 30.2 to 30.4‰ for Li6-N and Li7-N, respectively.[6,7,38] The Cambridge-1 Mg standard yields a long-term average δ^{26}Mg value of −2.62 ± 0.07‰ (2σ, *n* = 31), identical to published values (e.g.[4,34,41,45]). Seawater processed through the columns gives mean δ^{7}Li values of 31.27 ± 0.40‰ (2σ, *n* = 30 times through columns) and δ^{26}Mg values of −0.83 ± 0.05‰ (2σ, *n* = 25 times through columns), indistinguishable from accepted values of 31.0 ± 0.5‰ (e.g.[45]) and −0.83 ± 0.09‰.[46,47]

3.2.1 | δ^{7}Li and δ^{26}Mg values of standard reference materials

The isotopic ratios of Li and Mg are widely used within the geosciences, with application to both low- and high-temperature geochemical processes. Column chromatography methods are usually adapted to the preferred type of sample matrix with rock and sediment samples, with a high cationic content, requiring careful handling during column elution. To validate the column protocol and analytical technique described in this study we analysed a set of geological reference standards with published Li and Mg isotopic compositions. The results are in excellent agreement with published and accepted values (Tables 5 and 6).

TABLE 5 δ^{7}Li values of multiple reference standards

	δ^{7}Li (‰)	2σ (‰)	*n*	Loaded mass (ng)	Reference
BIR-1	**3.49**	**0.01**	**1**	**2**	**This study**
Basalt	3.30	0.60	5		54
	3.39	0.77	9		55
	3.9	1	4		56
BCR-2	**2.82**	**0.13**	**2**	**1-2**	**This study**
Basalt	3.50	0.20	22		54
	3.10	0.90	9		57
	2.6	0.3	18	10	58
	2.6	0.3	19	10	59
BHVO-2	**4.76**	**0.29**	**6**	**1-2**	**This study**
Basalt	4.40	0.80	11		57
	4.9	1.04	11	374	60
	4.7	0.2	31	10	59
	4.2	0.5	17		61
	4.7	0.2	31	10	15
	4.5	0.27	13		62
	4.8	0.2	15		63
SGR-1b	**4.96**	**0.62**	**6**	**2-5**	**This study**
Shale	3.6	0.4	3	20	64
	4.73	0.7	3	200-400	65
JCp-1	**20.27**	**0.41**	**4**	**0.3**	**This study**
Aragonite	20.16	0.2	5	1.2	24
Seawater	**31.27**	**0.4**	**30**	**0.3-5**	**This study**
	30.55	0.45	15	-	66
	30.88	0.12	46	1.2	24
	31.01	0.54	90	1	9
	31.1	0.2	31	2	31
	31.2	1.8	28	3-15	67
	31.8	1.9	15	40	26

n is the number of analyses, which equals the number of column separations for this study. Studies using MC-ICPMS are preferentially referenced for comparison. In addition, for commonly used standards, studies with 10 or more analyses are included (for a more comprehensive list of references, see http://georem.mpch-mainz.gwdg.de).

4 | DISCUSSION

4.1 | Plasma-based $^{12}C^{14}N^{+}$-interference on ^{26}Mg

Accurate determination of Mg isotope ratios may suffer from isobaric interference of carbon nitride, $^{12}C^{14}N^{+}$, on ^{26}Mg (Teng and Yang[41]) (Figure 5A). All the Mg measurements in this study were performed in medium resolution with an offset of the H1 cup (first high mass cup, used for the determination of ^{26}Mg) towards a higher mass (Figure 5). The CN interference sits on the right-hand shoulder of the ^{26}Mg-peak and an offset of the H1 cup towards a higher mass, combined with peak-centering on ^{25}Mg, quantitatively avoids the CN interference on ^{26}Mg.

4.2 | Sample-standard concentration matching

Several studies have highlighted the importance of accurate concentration matching between samples and the bracketing standard during isotope analysis. Instrumental backgrounds with very light δ^{7}Li compositions (−200‰) have been shown to cause analytical artefacts on measured ^{7}Li/^{6}Li when the concentrations of the bracketing standard and sample have deviated by more than 50%.[24,48-50]

TABLE 6 δ^{26}Mg and δ^{25}Mg values of multiple reference standards

	δ^{26}Mg (‰)	2σ (‰)	δ^{25}Mg (‰)	2σ (‰)	*n*	Reference
BIR-1	**−0.31**	**0.04**	**−0.17**	**0.05**	**2**	**This study**
Basalt	−0.22	0.06	−0.10	0.02	11	68
	−0.27	0.33	−0.18	0.18	14	69
	−0.29	0.01	−0.15	0.01	16	70
BCR-2	**−0.26**	**0.02**	**−0.13**	**0.05**	**4**	**This study**
Basalt	−0.16	0.01	−0.08	0.02	35	68
	−0.26	0.08	−0.13	0.05	54	71
	−0.32	0.15	−0.16	0.07	12	72
	−0.30	0.19	−0.16	0.11	31	69
	−0.26	0.13	−0.13	0.07	134	73
	−0.30	0.11	−0.15	0.07	18	41
	−0.30	0.08	−0.16	0.09	28	74
	−0.19	0.07	−0.09	0.07	15	70
BHVO-2	**−0.26**	**0.07**	**−0.14**	**0.04**	**6**	**This study**
Basalt	−0.22	0.04	−0.10	0.03	14	68
	−0.20	0.07	−0.10	0.05	54	71
	−0.31	0.19	−0.16	0.11	30	69
	−0.19	0.07	−0.10	0.03	10	75
AGV-2	**−0.16**	**0.08**	**−0.08**	**0.05**	**3**	**This study**
Andesite	−0.12	0.03	−0.06	0.03	19	68
	−0.24	0.24	−0.14	0.13	28	69
	−0.22	0.18	−0.12	0.08	15	73
G2	**−0.08**	**0.02**	**−0.03**	**0.04**	**1**	**This study**
Granite	−0.15	0.07	−0.08	0.06	12	44
	−0.13	0.05	−0.07	0.04	34	68
	−0.22	0.25	−0.07	0.14	16	41
SDC-1	**−0.07**	**0.02**	**−0.03**	**0.01**	**1**	**This study**
Mica schist	−0.11	0.03	−0.06	0.05	4	44
Sco-1	**−0.85**	**0.05**	**−0.43**	**0.01**	**3**	**This study**
Shale	−0.91	0.04	−0.48	0.03	-	76
	−0.89	0.08	−0.47	0.05	4	44
	−0.94	0.08	−0.50	0.06	1	77
SGR-1b	**−0.97**	**0.03**	**−0.52**	**0.03**	**3**	**This study**
Shale	−1.00	0.08	−0.51	0.03	4	44
	−0.98	0.12	−0.50	0.06	3	78
JCp-1	**−2.00**	**0.12**	**−1.05**	**0.07**	**25**	**This study**
Aragonite	−2.02	0.11	−1.05	0.06	15	79
	−2.01	0.22	−1.05	0.12	37	78
Seawater	**−0.83**	**0.05**	**−0.43**	**0.02**	**25**	**This study**
	−0.84	0.06	−0.43	0.04	102	44
	−0.83	0.11	−0.43	0.06	49	47
	−0.82	0.01	−0.43	0.01	26	46

n is the number of analyses, which equals the number of column separations for this study. Studies using MC-ICPMS are preferentially referenced for comparison. In addition, for commonly used standards, studies with 10 or more analyses are included (for a more comprehensive list of references, see http://georem.mpch-mainz.gwdg.de).

Concentrations of samples and standards were therefore matched to within ±10% of each other in this study. Especial care was taken for Li as the ^{7}Li beam intensities were close to the saturation voltage of the amplifiers (0.51 V with 10^{13} Ω resistors). To test the effects of mismatched concentrations of our instrumental method, L-SVEC was measured at varying concentrations against the bracketing L-SVEC standard (Figure 6). The resulting δ^{7}Li values remain within the external precision of the Li method (±0.39‰) for all tested sample/standard concentration ratios (Figure 6). However, the large mass bias observed for the raw δ^{7}Li values (e.g. −10‰ at sample/standard ratio of 0.5) confirms previous studies showing that instrumental backgrounds have light δ^{7}Li compositions.[24,48-50] Further, it highlights the importance of accurate blank correction.

4.3 | Matrix element effects

The presence of matrix elements in the analyte may degrade the accuracy of Mg isotope ratio determinations in dry plasma conditions (e.g.[22,41,42]), although instrumental mass bias in wet plasma appears to be less sensitive.[15,51,52] Matrix-induced mass bias is similarly recognised for Li isotope ratio determinations, especially when dry plasma is generated using an Aridus® membrane-containing desolvator.[31,49] The presence of matrix elements with intensities twice that of the Li beam has shown detectable changes in mass fractionation characterised by a decrease in δ^{7}Li values by up to 3‰.[26,32] However, the use of ESI® APEX-IR as a desolvator has been shown to produce stable δ^{7}Li values of L-SVEC doped with Mg, Al or Na up to ten times the concentration of Li.[24] As Li is measured at very low concentrations/voltages in this study the presence of small amounts of contaminant elements can have a disproportionate effect. Samples analysed for Li and Mg isotopes were therefore scanned for contamination from Na, Al, Ca and Fe prior to isotope analysis, and always had amounts indistinguishable from those of the bracketing standard and wash solution. However, to test the effects of possible contamination, matrix element doped solutions of L-SVEC and DSM-3 at contaminant/sample ratios of 0.1, 0.5, 1 and 2 were analysed against pure L-SVEC and DSM-3 solutions (Figures 7A and 8A). Elements that elute close to the Li and Mg peaks during column separation were prioritised for the doping test. In addition, Mg doping for Li was carried out, as Mg is a common contaminant in plastic vials.

Several 0.5 ppb L-SVEC solutions were individually doped with Na, Mg, Al and Ti (single-element high-purity ICPMS standards) at concentrations of 0.25, 0.50 and 1.0 ppb, with resulting contaminant/Li ratios ranging from 0.5 to 2. The introduction of matrix elements (0.25 ppb, 50% of the measured Li concentration) caused a decrease and destabilisation in the ^{7}Li/^{6}Li ratio of the bracketing contaminant-free L-SVEC standard (Figure 8A). The shift in mass bias could be caused by a change in the surface chemistry of the Apex and subsequent re-equilibration, or an initial increase in secondary ionisation of Li off the skimmer cone as a result of substitution of Li by matrix elements; however, this is speculative as further tests were not carried out. The lowering of the ^{7}Li/^{6}Li ratio of the bracketing standard coupled with biased transmission of ^{7}Li in the matrix-doped solutions (possibly due to increased space-charge effects) led to the initial δ^{7}Li value of matrix-doped L-SVEC being ~ +1‰ higher than the true value. However, the system re-equilibrated after ca 3 h analysis time, with the δ^{7}Li values being within the external precision of our method even at contaminant/Li ratios of 2. The destabilisation that occurred at the first introduction of contaminant elements highlights the importance

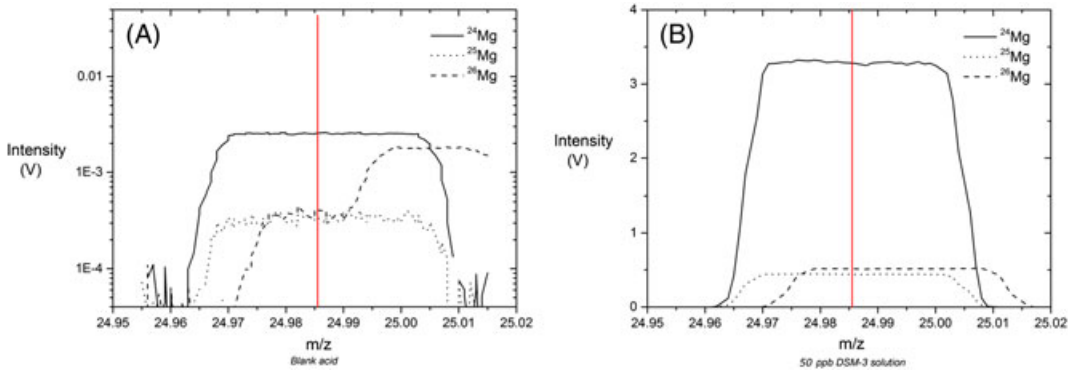

FIGURE 5 Offset H1 cup (^{26}Mg) towards higher mass to avoid CN interference. (A) CN interference (~0.9 mV) seen in blank acid, located on the right hand shoulder of the ^{26}Mg peak (dashed line). (B) Peak-centering (red vertical line) is performed in DSM-3 standard on ^{25}Mg (dotted line) [Color figure can be viewed at wileyonlinelibrary.com]

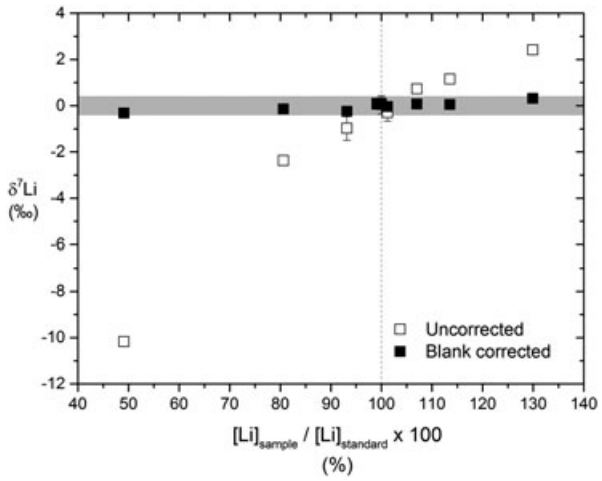

FIGURE 6 Uncorrected (open squares) and blank corrected (filled squares) δ^7Li values of L-SVEC with varying sample/standard concentration ratios. The grey field marks the external reproducibility in this study (±0.39‰). Blank corrected values all fall within this field

of careful sample handling during chemical purification and preparation, as a small amount of matrix elements may have a long lasting effect before re-equilibration occurs. We also observe no systematic offset in the measured δ^7Li values driven by the choice of doping element.

To test the effects of matrix element contamination on Mg isotopic ratios, DSM-3 at 100 ppb was doped with Na, Ca, Mn and Fe at 10, 100 and 200 ppb yielding contaminant/Mg ratios of 0.1, 1 and 2. We observe that the scatter in the measured Mg isotope ratio increased with the addition of contaminant elements (Figures 7B and 8B). The presence of Na lowers the δ^{26}Mg value, whereas Fe appears to increase the measured δ^{26}Mg value, although we did not observe any discernible trend in δ^{26}Mg values with the added mass of elements. Addition of Mn and Ca has no effect on the average δ^{26}Mg value at the concentrations utilised in the present experiment. However, the instrumental precision is reduced with the addition of the matrix elements, especially Ca. The values for the doped DSM-3 solutions do not deviate significantly from the mass-dependent fractionation line (with Δ^{25}Mg' values[53] within ±0.04, grey field in Figure 9), and Ca concentrations up to 200 ppb did not cause systematic interference

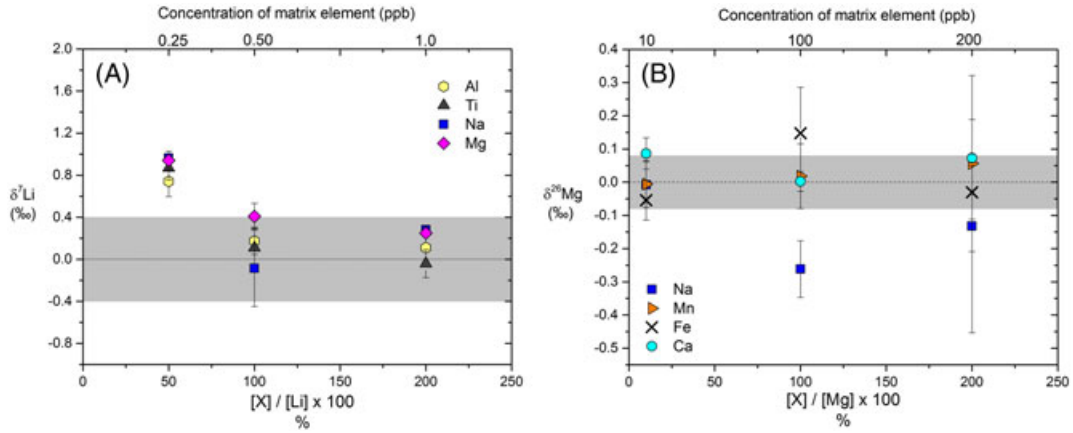

FIGURE 7 Effect of contaminant matrix elements on (A) δ^7Li values of L-SVEC and (B) δ^{26}Mg values of DSM-3. Li was analysed at 0.5 ppb and Mg at 100 ppb in this test. All values are blank corrected by subtracting the measured value of the blank preceding and following each sample and standard. The grey fields mark the external reproducibility in this study (±0.39‰ for δ^7Li measurements and ±0.07‰ for δ^{26}Mg measurements) [Color figure can be viewed at wileyonlinelibrary.com]

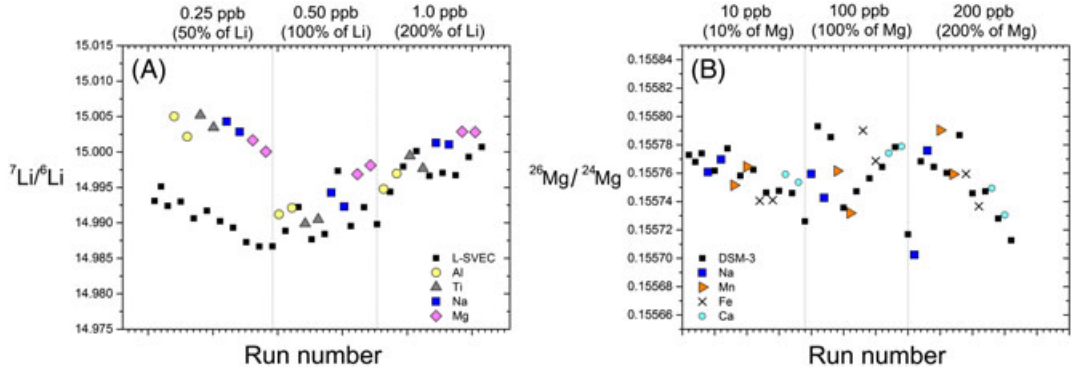

FIGURE 8 Effect of contaminant matrix elements on (A) δ^{7}Li values of L-SVEC and (B) δ^{26}Mg values of DSM-3 with run number during the analytical sequence. Li was analysed at 0.5 ppb and Mg at 100 ppb in this test. All values are blank corrected by subtracting the measured value of the blank preceding and following each sample and standard. See text for discussion [Color figure can be viewed at wileyonlinelibrary.com]

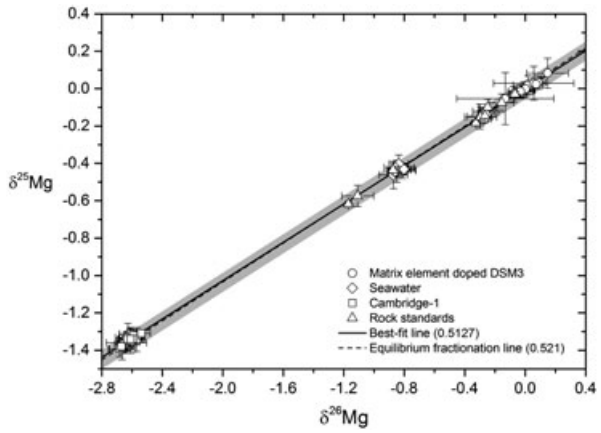

FIGURE 9 A cross plot of δ^{25}Mg and δ^{26}Mg values of samples analysed in this study.[53] The solid black line is the best-fit linear regression through the data set (slope = 0.5127, R^2 = 0.9997) and the dashed line is the theoretical equilibrium fractionation line[53] (slope = 0.521). DSM-3 solutions doped with matrix elements (circles) do not show observable deviation from the regression line but do, however, suffer from larger instrumental uncertainty than other purified samples

on ^{24}Mg when the ratios were measured in medium resolution. The results from both the Li and the Mg experiments highlight the importance of quantitative separation during column separation, and care during post-column processing.

5 | CONCLUSIONS

A single-step cation-exchange column method has been established for the combined separation of trace levels of Li and Mg from natural sample matrices. We utilise the high separation factors between Li and Na, Mg and Fe, Mn and K, in the macro-porous resin AGMP-50, combined with a high aspect ratio column for the quantitative separation of Li and Mg after a single elution. The cumulative blanks are low (<4 pg Li and <1 ng Mg) allowing sub-nanogram amounts of Li to be processed. Li was typically loaded at between 0.3 and 20 ng yielding Mg masses between 1 and 70 μg. Li and Mg isotopic ratios were measured by MC-ICPMS on the Thermo Scientific™ NEPTUNE *Plus*™. Li isotope analyses were performed utilising 10^{13} Ω amplifiers on the Faraday collectors, which allowed accurate and precise determination of isotopic ratios at ^{7}Li ion beams of <0.51 V, with a total sample consumption of <0.5 ng Li per duplicate analysis. Mg was measured in medium resolution with 10^{11} Ω amplifiers at ~10 V signal on ^{24}Mg with a total sample consumption of <115 ng Mg per duplicate analysis. The long-term external precision (2σ) is ±0.39‰ and ±0.07‰ for δ^{7}Li and δ^{26}Mg values, respectively, determined by repeated measurements over 18 months of secondary standards (Li6-N, Li7-N and Cambridge-1). The δ^{7}Li and δ^{26}Mg values obtained for several geological reference standards are in excellent agreement with published values. Seawater has been eluted with Li masses ranging from 0.3 to 5 ng, yielding an average δ^{7}Li value of 31.27 ± 0.40‰ (n = 30) and δ^{26}Mg value of −0.83 ± 0.05‰ (n = 25). The possibility of eluting small masses and the low analytical sample consumption make this method ideal for samples of limited mass or low Li concentration, such as foraminifera, mineral separates or dilute river waters.

ACKNOWLEDGEMENTS

We thank Albert Galy for the DSM-3 and Cambridge-1 Mg standards used in this study, and Nathalie Vigier for the Li6-N and Li7-N Li standards. Martijn Bökkerink is gratefully thanked for assisting with column calibrations. Ed Tipper is thanked for helpful comments on the manuscript. This project is supported in the framework of the Initial Training Network (ITN) iTECC funded by the EU REA under the FP7 implementation of the Marie Curie Action, under grant agreement number 316966, NERC grants NE/P011659/1, NE/N007441/1 and ERC Grant 2010-NEWLOG ADG-267931 HE.

ORCID

Madeleine S. Bohlin http://orcid.org/0000-0002-2101-9005
Nicholas Lloyd http://orcid.org/0000-0002-1359-0551
Mike J. Bickle http://orcid.org/0000-0001-8889-3410

REFERENCES

1. Chan LH, Edmond JM, Thompson G, Gillis K. Lithium isotopic composition of submarine basalts: Implications for the lithium cycle in the oceans. *Earth Planet Sci Lett*. 1992;108:151-160.

2. Kısakűrek B, James RH, Harris NBW. Li and δ^{7}Li in Himalayan rivers: Proxies for silicate weathering? *Earth Planet Sci Lett*. 2005;237:387-401.

3. Pogge von Strandmann PAE, Burton KW, James RH, van Calsteren P, Gíslason SR, Mokadem F. Riverine behaviour of uranium and lithium isotopes in an actively glaciated basaltic terrain. *Earth Planet Sci Lett*. 2006;251:134-147.
4. Tipper ET, Galy A, Gaillardet J, Bickle MJ, Elderfield H, Carder EA. The magnesium isotope budget of the modern ocean: Constraints from riverine magnesium isotope ratios. *Earth Planet Sci Lett*. 2006;250:241-253.
5. Tipper ET, Calmels D, Gaillardet J, Louvat P, Capmas F, Dubacq B. Positive correlation between Li and Mg isotope ratios in the river waters of the Mackenzie Basin challenges the interpretation of apparent isotopic fractionation during weathering. *Earth Planet Sci Lett*. 2012;333(/334):35-45.
6. Vigier N, Gislason SR, Burton KW, Millot R, Mokadem F. The relationship between riverine lithium isotope composition and silicate weathering rates in Iceland. *Earth Planet Sci Lett*. 2009;287:434-441.
7. Millot R, Vigier N, Gaillardet J. Behaviour of lithium and its isotopes during weathering in the Mackenzie Basin, Canada. *Geochim Cosmochim Acta*. 2010;74:3897-3912.
8. Teng FZ, Li WY, Rudnick RL, Gardner LR. Contrasting lithium and magnesium isotope fractionation during continental weathering. *Earth Planet Sci Lett*. 2010;300:63-71.
9. Misra S, Froelich PN. Lithium isotope history of Cenozoic seawater: Changes in silicate weathering and reverse weathering. *Science*. 2012;335:818-823.
10. Henchiri S, Clergue C, Dellinger M, Gaillardet J, Louvat P, Bouchez J. The influence of hydrothermal activity on the Li isotopic signature of rivers draining volcanic areas. *Procedia Earth Planet Sci*. 2014;10:223-230.
11. Zack T, Tomascak PB, Rudnick RL, Dalpé C, McDonough WF. Extremely light Li in orogenic eclogites: The role of isotope fractionation during dehydration in subducted oceanic crust. *Earth Planet Sci Lett*. 2003;208:279-290.
12. Elliott T, Jeffcoate A, Bouman C, Jeffcoate AB, Bouman C. The terrestrial Li isotope cycle: Light-weight constraints on mantle convection. *Earth Planet Sci Lett*. 2004;220:231-245.
13. Teng FZ, McDonough WF, Rudnick RL, et al. Lithium isotopic composition and concentration of the upper continental crust. *Geochim Cosmochim Acta*. 2004;68:4167-4178.
14. Teng FZ, Rudnick RL, McDonough WF, Gao S, Tomascak PB, Liu Y. Lithium isotopic composition and concentration of the deep continental crust. *Chem Geol*. 2008;255:47-59.
15. Pogge von Strandmann PAE, Elliott T, Marschall HR, et al. Variations of Li and Mg isotope ratios in bulk chondrites and mantle xenoliths. *Geochim Cosmochim Acta*. 2011;75:5247-5268.
16. Young ED, Galy A. The isotope geochemistry and cosmochemistry of magnesium. *Rev Mineral Geochem*. 2004;55:197-230.
17. Magna T, Wiechert UH, Halliday AN. New constraints on the lithium isotope compositions of the moon and terrestrial planets. *Earth Planet Sci Lett*. 2006;243:336-353.
18. Wiechert UH, Halliday AN. Non-chondritic magnesium and the origins of the inner terrestrial planets. *Earth Planet Sci Lett*. 2007;256:360-371.
19. Bigeleisen J. Chemistry of isotopes: Isotope chemistry has opened new areas of chemical physics, geochemistry, and molecular biology. *Science*. 1965;147:463-471.
20. Tomascak PB. Developments in the understanding and application of lithium isotopes in the earth and planetary sciences. *Rev Mineral Geochem*. 2004;55:153-195.
21. Teng FZ. Magnesium isotope geochemistry. *Rev Mineral Geochem*. 2017;82:219-287.
22. Galy A, Belshaw NS, Halicz L, O'Nions RK. High-precision measurement of magnesium isotopes by multiple-collector inductively coupled plasma mass spectrometry. *Int J Mass Spectrom*. 2001;208:89-98.
23. Misra S, Froelich PN. Measurement of lithium isotope ratios by quadrupole-ICP-MS: Application to seawater and natural carbonates. *J Anal At Spectrom*. 2009;24:1524-1533.
24. Huang KF, You CF, Liu YH, Wang RM, Lin PY, Chung CH. Low-memory, small sample size, accurate and high-precision determinations of lithium isotopic ratios in natural materials by MC-ICP-MS. *J Anal At Spectrom*. 2010;25:1019-1024.
25. Moriguti T, Nakamura E. High-yield lithium separation and the precise isotopic analysis for natural rock and aqueous samples. *Chem Geol*. 1998;145:91-104.
26. Tomascak PB, Carlson RW, Shirey SB. Accurate and precise determination of Li isotopic compositions by multi-collector sector ICP-MS. *Chem Geol*. 1999;158:145-154.
27. James RH, Palmer MR. The lithium isotope composition of international rock standards. *Chem Geol*. 2000;166:319-326.
28. Chang VTC, Makishima A, Belshaw NS, O'Nions RK. Purification of Mg from low-Mg biogenic carbonates for isotope ratio determination using multiple collector ICP-MS. *J Anal At Spectrom*. 2003;18:296-301.
29. Strelow FWE, Van Zyl CR, Bothma CJC. Distribution coefficients and the cation-exchange behaviour of elements in hydrochloric acid-ethanol mixtures. *Anal Chim Acta*. 1969;45:81-92.
30. Jeffcoate AB, Elliott T, Thomas A, Bouman C. Precise, small sample size determinations of lithium isotopic compositions of geological reference materials and modern seawater by MC-ICP-MS. *Geostand Geoanal Res*. 2004;28:161-172.
31. Nishio Y, Nakai SS. Accurate and precise lithium isotopic determinations of igneous rock samples using multi-collector inductively coupled plasma mass spectrometry. *Anal Chim Acta*. 2002;456:271-281.
32. Strelow FWE, Weinert CHSW, Van Der Walt TN. Separation of lithium from sodium, beryllium and other elements by cation-exchange chromatography in nitric acid-methanol. *Anal Chim Acta*. 1974;71:123-132.
33. Tipper ET, Galy A, Bickle MJ. Calcium and magnesium isotope systematics in rivers draining the Himalaya-Tibetan-Plateau region: Lithological or fractionation control? *Geochim Cosmochim Acta*. 2008;72:1057-1075.
34. Strelow FWE. Distribution coefficients and cation-exchange behaviour of 45 elements with a macroporous resin in hydrochloric acid/methanol mixtures. *Anal Chim Acta*. 1984;160:31-45.
35. Strelow FWE. Distribution coefficients and ion exchange behaviour of some chloride complex forming elements with Bio Rad AG50W-Xb cation exchange resin in mixed nitric-hydrochloric acid solutions. *Solvent Extr Ion Exch*. 1989;7:735-747.
36. Tipper ET, Louvat P, Capmas F, Galy A, Gaillardet J. Accuracy of stable Mg and Ca isotope data obtained by MC-ICP-MS using the standard addition method. *Chem Geol*. 2008;257:65-75.
37. Flesch GD, Anderson JRAR, Svec HJ. A secondary isotopic standard for $^{6}Li/^{7}Li$ determinations. *Int J Mass Spectrom Ion Phys*. 1973;12:265-272.
38. Carignan J, Vigier N, Millot R. Three secondary reference materials for lithium isotope measurements : Li7-N, Li6-N and LiCl-N solutions. *Geostand Geoanal Res*. 2007;31:7-12.
39. Lin J, Liu Y, Hu Z, et al. Accurate determination of lithium isotope ratios by MC-ICP-MS without strict matrix-matching by using a novel washing method. *J Anal At Spectrom*. 2016;31:390-397.
40. Galy A, Yoffe O, Janney PE, et al. Magnesium isotope heterogeneity of the isotopic standard SRM980 and new reference materials for magnesium-isotope-ratio measurements. *J Anal At Spectrom*. 2003;18:1352-1356.
41. Teng FZ, Yang W. Comparison of factors affecting the accuracy of high-precision magnesium isotope analysis by multi-collector inductively coupled plasma mass spectrometry. *Rapid Commun Mass Spectrom*. 2014;28:19-24.
42. Taylor TI, Urey HC. Fractionation of the lithium and potassium isotopes by chemical exchange with zeolites. *J Chem Phys*. 1938;6:429-438.
43. Teng FZ, Li WY, Ke S, et al. Magnesium isotopic compositions of international geological reference materials. *Geostand Geoanal Res*. 2015;39:329-339.
44. Huang F, Glessner J, Ianno A, Lundstrom C, Zhang Z. Magnesium isotopic composition of igneous rock standards measured by MC-ICP-MS. *Chem Geol*. 2009;268:15-23.

45. Tomascak PB. Developments in the understanding and application of lithium isotopes in the earth and planetary sciences. *Rev Mineral Geochem*. 2004;55:153-195.
46. Foster GL, Pogge Von Strandmann PAE, Rae JWB. Boron and magnesium isotopic composition of seawater. *Geochem Geophys Geosyst*. 2010;11:1-10.
47. Ling MX, Sedaghatpour F, Teng FZ, Hays PD, Strauss J, Sun W. Homogeneous magnesium isotopic composition of seawater: An excellent geostandard for Mg isotope analysis. *Rapid Commun Mass Spectrom*. 2011;25:2828-2836.
48. Bryant CJ, McCulloch MT, Bennett VC. Impact of matrix effects on the accurate measurement of Li isotope ratios by inductively coupled plasma mass spectrometry (MC-ICP-MS) under "cold" plasma conditions. *J Anal At Spectrom*. 2003;18:734-737.
49. Magna T, Wiechert UH, Halliday AN. Low-blank isotope ratio measurement of small samples of lithium using multiple-collector ICPMS. *Int J Mass Spectrom*. 2004;239:67-76.
50. Rosner M, Ball L, Peucker-Ehrenbrink B, Blusztajn J, Bach W, Erzinger J. A simplified, accurate and fast method for lithium isotope analysis of rocks and fluids, and δ^7Li values of seawater and rock reference materials. *Geostand Geoanal Res*. 2007;31:77-88.
51. Teng FZ, Li WY, Ke S, et al. Magnesium isotopic composition of the earth and chondrites. *Geochim Cosmochim Acta*. 2010;74:4150-4166.
52. Wang G, Lin Y, Liang X, et al. Separation of magnesium from meteorites and terrestrial silicate rocks for high-precision isotopic analysis using multiple collector-inductively coupled plasma-mass spectrometry. *J Anal At Spectrom*. 2011;26:1878-1886.
53. Young ED, Galy A, Nagahara H. Kinetic and equilibrium mass-dependent isotope fractionation laws in nature and their geochemical and cosmochemical significance. *Geochim Cosmochim Acta*. 2002;66:1095-1104.
54. Ryu JS, Vigier N, Lee SW, Lee KS, Chadwick OA. Variation of lithium isotope geochemistry during basalt weathering and secondary mineral transformations in Hawaii. *Geochim Cosmochim Acta*. 2014;145:103-115.
55. Schuessler JA, Schoenberg R, Sigmarsson O. Iron and lithium isotope systematics of the Hekla volcano, Iceland - Evidence for Fe isotope fractionation during magma differentiation. *Chem Geol*. 2009;258:78-91.
56. Rudnick RL, Tomascak PB, Njo HB, Gardner LR. Extreme lithium isotopic fractionation during continental weathering revealed in saprolites from South Carolina. *Chem Geol*. 2004;212:45-57.
57. Genske FS, Turner SP, Beier C, et al. Lithium and boron isotope systematics in lavas from the Azores islands reveal crustal assimilation. *Chem Geol*. 2014;373:27-36.
58. Pogge von Strandmann PAE, Opfergelt S, Lai YJ, Sigfússon B, Gislason SR, Burton KW. Lithium, magnesium and silicon isotope behaviour accompanying weathering in a basaltic soil and pore water profile in Iceland. *Earth Planet Sci Lett*. 2012;339–340:11-23.
59. Penniston-Dorland SC, Bebout GE, Pogge von Strandmann PAE, Elliott T, Sorensen SS. Lithium and its isotopes as tracers of subduction zone fluids and metasomatic processes: Evidence from the Catalina Schist, California, USA. *Geochim Cosmochim Acta*. 2012;77:530-545.
60. Brant C, Coogan LA, Gillis KM, Seyfried WE, Pester NJ, Spence J. Lithium and Li-isotopes in young altered upper oceanic crust from the East Pacific Rise. *Geochim Cosmochim Acta*. 2012;96:272-293.
61. Vlastélic I, Staudacher T, Bachèlery P, Télouk P, Neuville D, Benbakkar M. Lithium isotope fractionation during magma degassing: Constraints from silicic differentiates and natural gas condensates from Piton de la Fournaise volcano (Réunion Island). *Chem Geol*. 2011;284:26-34.
62. Magna T, Ionov DA, Oberli F, Wiechert UH. Links between mantle metasomatism and lithium isotopes: Evidence from glass-bearing and cryptically metasomatized xenoliths from Mongolia. *Earth Planet Sci Lett*. 2008;276:214-222.
63. Marschall HR, Pogge von Strandmann PAE, Seitz HM, Elliott T, Niu Y. The lithium isotopic composition of orogenic eclogites and deep subducted slabs. *Earth Planet Sci Lett*. 2007;262:563-580.
64. Pogge von Strandmann PAE, Frings PJ, Murphy MJ. Lithium isotope behaviour during weathering in the Ganges Alluvial Plain. *Geochim Cosmochim Acta*. 2017;198:17-31.
65. Phan TT, Capo RC, Stewart BW, Macpherson GL, Rowan EL, Hammack RW. Factors controlling Li concentration and isotopic composition in formation waters and host rocks of Marcellus Shale, Appalachian Basin. *Chem Geol*. 2016;420:162-179.
66. Choi MS, Ryu J, Park Y, et al. Precise determination of the lithium isotope ratio in geological samples using MC-ICP-MS with cool plasma. *J Anal At Spectrom*. 2013;28:505-509.
67. Millot R, Guerrot C, Vigier N. Accurate and high-precision measurement of lithium isotopes in two reference materials by MC-ICP-MS. *Geostand Geoanal Res*. 2004;28:153-159.
68. An Y, Wu F, Xiang Y, et al. High-precision Mg isotope analyses of PT US CR. *Chem Geol*. 2014;390:9-21.
69. Opfergelt S, Georg RB, Delvaux B, Cabidoche Y, Burton KW, Halliday AN. Mechanisms of magnesium isotope fractionation in volcanic soil weathering sequences, Guadeloupe. *Earth Planet Sci Lett*. 2012;341–344:176-185.
70. Baker J, Bizzarro M, Wittig N, Connelly J, Haack H. Early planetesimal melting from an age of 4.5662 Gyr for differentiated meteorites. *Nature*. 2005;436:1127-1131.
71. Lee SW, Ryu JS, Lee KS. Magnesium isotope geochemistry in the Han River, South Korea. *Chem Geol*. 2014;364:9-19.
72. Bouvier A, Wadhwa M, Simon SB, Grossman L. Magnesium isotopic fractionation in chondrules from the Murchison and Murray CM2 carbonaceous chondrites. *Meteorit Planet Sci*. 2013;48:339-353.
73. Chopra R, Richter FM, Watson EB, Scullard CR. Magnesium isotope fractionation by chemical diffusion in natural settings and in laboratory analogues. *Geochim Cosmochim Acta*. 2012;88:1-18.
74. Teng FZ, McDonough WF, Rudnick RL, Wing BA. Limited lithium isotopic fractionation during progressive metamorphic dehydration in metapelites: A case study from the Onawa contact aureole, Maine. *Chem Geol*. 2007;239:1-12.
75. Bizzarro M, Paton C, Larsen K, Schiller M, Trinquier A, Ulfbeck D. High-precision Mg-isotope measurements of terrestrial and extraterrestrial material by HR-MC-ICPMS – Implications for the relative and absolute Mg-isotope composition of the bulk silicate earth. *J Anal At Spectrom*. 2011;26:565-577.
76. Ma L, Teng FZ, Jin L, et al. Magnesium isotope fractionation during shale weathering in the Shale Hills Critical Zone Observatory: Accumulation of light Mg isotopes in soils by clay mineral transformation. *Chem Geol*. 2015;397:37-50.
77. Li WY, Teng FZ, Ke S, et al. Heterogeneous magnesium isotopic composition of the upper continental crust. *Geochim Cosmochim Acta*. 2010;74:6867-6884.
78. Wombacher F, Eisenhauer A, Heuser A, Weyer S. Separation of Mg, Ca and Fe from geological reference materials for stable isotope ratio analyses by MC-ICP-MS and double-spike TIMS. *J Anal At Spectrom*. 2009;24:627-636.
79. Planchon F, Poulain C, Langlet D, Paulet YM, André L. Mg-isotopic fractionation in the manila clam (*Ruditapes philippinarum*): New insights into Mg incorporation pathway and calcification process of bivalves. *Geochim Cosmochim Acta*. 2013;121:374-397.

How to cite this article: Bohlin MS, Misra S, Lloyd N, Elderfield H, Bickle MJ. High-precision determination of lithium and magnesium isotopes utilising single column separation and multi-collector inductively coupled plasma mass spectrometry. *Rapid Commun Mass Spectrom*. 2018;32:93-104. https://doi.org/10.1002/rcm.8020